Clean synthesis of linear and star amphiphilic poly(ε-caprolactone)-*block*-poly (ethyl ethylene phosphonate) block copolymers: assessing self-assembly and surface activity

Payal Baheti,[a,b] Timo Rheinberger,[c] Olinda Gimello,[a] Cécile Bouilhac,[a*] Frederik R. Wurm,[c] Patrick Lacroix-Desmazes,[a*] Steven M. Howdle[b*]

[a] ICGM, Univ. Montpellier, CNRS, ENSCM, Montpellier, France
[b] School of Chemistry, University of Nottingham, University Park, Nottingham NG7 2RD, United Kingdom
[c] Max-Planck-Institut für Polymerforschung, Ackermannweg 10, 55128 Mainz, Germany.

*Corresponding author e-mail: *cecile.bouilhac@umontpellier.fr*,
patrick.lacroix-desmazes@enscm.fr, *steve.howdle@nottingham.ac.uk*

Abstract

Anionic ring-opening polymerization (AROP) of 2-ethyl-2-oxo-1,3,2-dioxaphospholane (EP) has been utilized to create alternative hydrophilic moieties for utilization in surfactants. The current "go-to" hydrophilic unit is poly(ethyleneglycol) (PEG), but this is non-biodegradable and there is some evidence that their use can lead to accumulation of toxic by-products. We have created new approaches leading to water-dispersible, fully degradable amphiphilic block copolymers. Our approach utilized poly(ε-caprolactone)-based macroinitiators in a solvent free process with organocatalyst DBU. We have prepared a comprehensive set of novel amphiphilic PCL-*b*-PEP block copolymers including linear diblock, triblock and star diblock copolymers characterized by SEC, ^{1}H and ^{31}P NMR and MALDI-TOF analyses. Supercritical carbon dioxide (scCO$_2$) was exploited to efficiently extract the residual EP monomer leading to significantly increased gravimetric yields of purified product compared to conventional techniques such as dialysis. The self-assembly of the amphiphilic copolymers in water was investigated by DLS and cryo-TEM and their surface-activity as a function of concentration was investigated by tensiometry showing behavior that matches or exceeds commercially available surfactants.
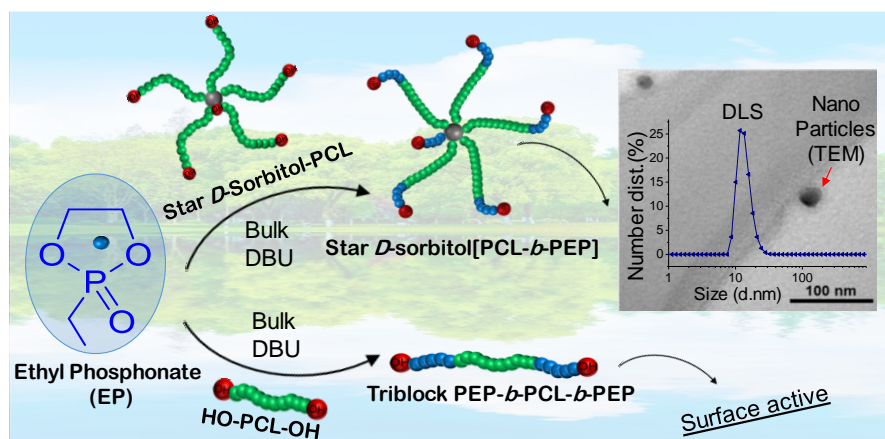
Keywords. *Star polymers, block copolymers, polycaprolactone, polyphosphoester, supercritical carbon dioxide, self-assembly, unimolecular micelles, and macromolecular surfactants.*

1. Introduction

Stringent environmental regulations and political frameworks will require a shift towards utilisation of sustainable and biodegradable surfactants in the personal care industry and for this reason there is strong interest in developing new surfactants.[1] We present a unique approach to new surfactant architectures based upon linear and star polymers, developed from natural resources; ensuring they are both amphiphilic and degradable and utilizing eco-friendly processing systems.

Amphiphilic copolymers are ubiquitous in our lives; as laundry detergents, food additives, cosmetics or even medicines.[2] In an aqueous medium or selective solvent, they spontaneously self-assemble into discrete aggregates consisting of a solvophobic core and solvophilic shell (corona).[3,4] Such aggregates can develop into advanced morphologies such as micellar or vesicular[4] conformations that are useful in a wide range of applications; for example as nano-vehicles in the biomedical-pharmaceutical field.[5,6] Conventional linear amphiphiles generally form aggregates such as micelles above their critical aggregation concentration (CAC) where the morphology obtained depends on the solvophilicity of the primary structure (i.e. the composition of blocks, chain length, and sequence)[7] and on the concentration, temperature, solvent, and pH.[8] However for pharmaceutical applications, the high dilution that occurs upon injection into the bloodstream can cause disassembly of such nanocarriers and premature drug release[8–10] and hence there is a need for more robust systems.

One promising route is to exploit branched polymer systems. In sharp contrast to the linear block copolymeric micelles, branched structures are often characterized by the formation of "unimolecular micelles"[6,11–16] which cannot disassemble, thereby forming a monodisperse and structurally stable dispersed phase that is by its very nature not affected by dilution.[15,17–20] Examples of branched amphiphilic macromolecules include dendrimers,[10,18] hyperbranched,[10,21,22] and star polymers[8,10,20,21,23] which can possess different moieties of contrasting polarity, bound together in a covalently tethered three-dimensional core-shell system. The improved stability upon dilution of these unimolecular micelles arises from the fact that they are multiple linear polymers, covalently connected, so that disassembly is no longer possible.[24]

Star polymers are branched polymers with three or more arms of often similar lengths, radiating from a central core where the core may be an atom, a small molecule, or a macromolecular structure.[25] They have attracted significant attention because their properties are similar to dendrimers but they are much easier to access.[26–28] One prominent example is Tetronic® (commercialized by BASF) a four-arm star amphiphilic block copolymer [poly(ethylene oxide)-*block*-poly(propylene oxide) (star PEO-*b*-PPO)] used in the cosmetics, paper and petroleum industries.[29] Among all the star-like polymers, polyesters constitute an attractive class for drug delivery systems because of their potential biodegradability and biocompatiblity.[30] The hydrophobic segment is most commonly poly(lactic acid) (PLA), poly(ε-caprolactone) (PCL) or poly(glycolic acid).[6] However, a hydrophilic segment is also required[31] and poly(ethylene glycol) (PEG) is today's gold standard in the biomedical field[32] because it has high water solubility, low toxicity and low immunogenicity. However, PEG is non-biodegradable and there is some evidence of accumulation of toxic by-products from uncontrolled and undesirable oxidative degradation that have raised concerns.[33–36] Alternative hydrophilic polymers are being investigated and include poly(amino acid)s,[37,38] poly(2-oxazoline)s,[39–44] poly(peptoid)s,[45–47] and poly(phosphoester)s[48,49] (PPE)s and polyphosphonates.[50] The latter show considerable promise because they are water soluble, degradable and show promising cytotoxicity.[50,51]

The hydrolytic and enzymatic degradation of PPEs has been reported.[52] Especially polyphosphonates have proven to undergo hydrolytic degradation at physiological pH or under basic conditions.[53] Hydrolysis of phosphonate esters proceeds via a nucleophilic attack of water or hydroxyl ions to the phosphorous center[54] or by a backbiting mechanism.[55] The hydrolytic stability of polyphosphonates was found dependent of the nature of the alkyl side chain. Degradation times can be adjusted from hours to weeks at physiological pH for polymers with different side chains (e.g. methyl < ethyl < isopropyl).[50]

Could polyphosphonates provide a degradable alternative to PEG as the hydrophilic segment in unimolecular micelles? To the best of our knowledge, amphiphilic block copolymers containing poly(phosphonate) functional groups and hydrophobic polyesters (PCL or PLA) have not yet been reported, though previous studies have prepared gradient copolymers of PLA and PEP by direct copolymerization.[56]

We present a new approach to controlled synthesis of poly(ethyl ethylene phosphonate) (PEP) leading to a range of amphiphilic linear, diblock, triblock and star diblock copolymers containing hydrophilic polyphosphonate groups and hydrophobic polyesters (PCL-*b*-PEP) that are fully degradable (Figure 1). Our synthetic approach also exploits supercritical carbon dioxide (scCO$_2$) to ensure green synthesis and the removal of potentially toxic starting materials and by-products. The surface-activities of all the block copolymers are evaluated using the Wilhelmy plate method and dynamic light scattering (DLS) and transmission electron microscopy (TEM) are exploited to determine self-assembly and the ability to form micellar structures.
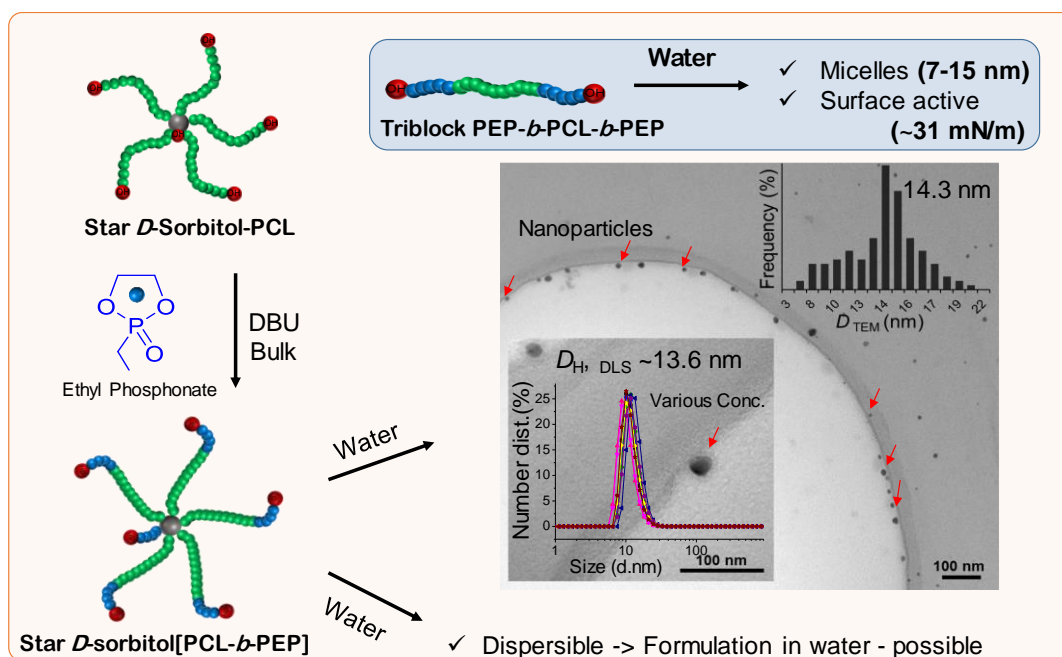

Figure 1. The eco-friendly route for the clean synthesis of amphiphilic star *D*-sorbitol[PCL-*b*-PEP] diblock copolymer from star *D*-sorbitol-PCL homopolymer and amphiphilic triblock copolymer PEP-*b*-PCL-*b*-PEP from hydroxy-telechelic homopolymer HO-PCL-OH.

2. Experimental Section

2.1. Synthesis of Linear or Star Polyol-PCL using Sn(Oct)$_2$ in Supercritical CO$_2$

The stainless steel high-pressure autoclave reactor (20 mL) used for polymer synthesis with scCO$_2$ has been described previously.[57] Star D-sorbitol[PCL-OH$_6$] was synthesized in scCO$_2$ using Sn(Oct)$_2$ as the catalyst following Baheti et al.[58] D-sorbitol (93.8 mg, 0.52 mmol) and 10 mol% of Sn(Oct)$_2$ (20.8 mg, 0.05 mmol) were loaded into the base of the autoclave and degassed with CO$_2$ at 3 bar to ensure removal of air. ε-Caprolactone (ε-CL, 3 ml, 27.07 mmol) was then added. The reactor was pressurized to 70 bar and gradually heated to 95 °C (10 °C/min). Subsequently, the pressure was increased to 240 bar CO$_2$ and the reaction was stabilized at 95 °C and 240 bar for 10 min. At this point, the reaction mixture was agitated using a mechanical stirrer at 300 rpm for 2.5 days. The gravimetric yield after polymerization was 96%. Polymer was precipitated in cold ethanol from THF solution and dried under vacuum). SEC-MALS (THF): $M_n^{\text{SEC-MALS}}$ = 6700 g/mol, $Đ$ = 1.04 (Table 1, Entry 3).
Analogously, low MW linear hydroxy terminated and dihydroxy telechelic PCL were synthesized using linear alcohols as initiators: benzyl alcohol (BzOH) and 1,6-hexanediol (HexD), in scCO$_2$ (95 °C, 240 bar). The analytical results are presented in Table 1.

2.2. Synthesis of PCL-b-PEP Diblock and Triblock Copolymer in the Bulk

A specific example of synthesis of poly(ε-caprolactone)-$block$-poly(ethyl phosphonate) (PCL$_n$-b-PEP$_m$) diblock copolymers (linear and star) by bulk AROP using DBU is described (Table 1, Entry 5-8). A linear Bz-PCL-b-PEP diblock copolymer of M_n^{targ} (PEP block) of 6100 g/mol (i.e. DP_n^{targ} = 45) was synthesized using linear benzyl-PCL-OH (Bz-PCL$_{19}$-OH) as a macroinitiator. Bz-PCL$_{19}$OH (85.6 mg, 3.72 × 10^{-2} mmol, M_n^{NMR} (macroinitiator) = 2300 g/mol, $Đ$ = 1.02, Table 1, Entry 1) and EP (227 mg, 1.67 mmol) were charged to a flame-dried Schlenk tube (3 mL), degassed with argon for 30 min while stirring (300 rpm). The Schlenk tube was homogenized at ~55-60 °C for 15-20 min. An aliquot was also withdrawn to ensure there is no initiation at this stage. The catalyst, DBU (5.6 mg, 3.72 × 10^{-2} mmol, 1.0 equimolar respect to hydroxy on the initiator) was added under an inert atmosphere and the polymerizations were conducted for 2 h for linear materials to reach monomer conversions of ~88-99% as monitored by ^{1}H NMR (Table 1, Entry 5). In general, polymers were purified either by dialysis to give a gravimetric yield of 62 ± 5% or by supercritical extraction to give a gravimetric yield of 92 ± 5 %. The linear triblock poly(ethyl phosphonate)-$block$-poly(caprolactone)-$block$-poly(ethyl phosphonate) (PEP$_m$-b-PCL$_n$-b-PEP$_m$) copolymers and star diblock copolymers were synthesized following the same procedure and the specified molar ratio of feedstock (Table 1, Entry 6-8).

2.2.1. Bz-PCL-b-PEP.
^{1}H NMR (400 MHz, DMSO-d_6). δ (ppm) 7.42 – 7.30 (m, aromatic proton), 5.08 (s, aryl –CH_2–), 4.86 (t, terminal –O–H), 4.43 – 4.22 (m, backbone, –CH_2–CH_2–), 3.99 (t, methylene ester –CH_2OCO– of PCL), 3.95 – 3.90 (m, broad, last methylene ester –CH_2OCO– of PCL and methylene in β position of terminal PEP –OP(=O)–CH_2–CH$_2$–OH), 3.74 (t, J = 5.2 Hz), 3.56 (m, terminal –CH_2–OH), 2.28 (t, methylene in α position to carbonyl group –CH_2–CO– of PCL), 1.84 – 1.64 (m, side-chain –P–CH_2–), 1.64 1.43 (m,–COCH$_2$CH_2CH$_2$CH_2CH$_2$O–), 1.36 1.20 (m, COCH$_2$CH$_2$CH_2CH$_2$CH$_2$O), 1.14 – 0.97 (m, side-chain –CH_3).

2.2.2. Star D-sorbitol[PCL$_n$-b-PEP$_m$].
^{1}H NMR (400 MHz, DMSO-d_6) δ (ppm) 4.85 (s, –OH), 4.43 4.22- (m, phosphonate backbone –CH_2CH_2–), 3.99 (t, methylene ester –CH_2OCO– of PCL), 3.96 – 3.87 (m, broad, last methylene ester –CH_2OCO– of PCL and methylene in β

position of terminal PEP –OP(=O)–CH_2–CH$_2$–OH), 3.55 (m,– CH_2– OH), 2.28 (t, methylene in α position to carbonyl of PCL –CH_2–CO), 1.84 – 1.64 (m, side-chain –P–CH_2–), 1.64 - 1.43 (m,–COCH$_2$CH_2CH$_2$CH_2CH$_2$O–), 1.36 1.20 (m, COCH$_2$CH$_2$CH_2CH$_2$CH$_2$O), 1.14 – 0.97 (m, side-chain –CH_3).

3. Results and Discussion

Our strategy was to prepare linear diblock and triblock copolymers and then to extend the technique to star block copolymers. Finally, we investigate the behavior of all the materials in aqueous solution.

3.1. Linear Diblock and Triblock copolymers
3.1.1. Synthesis

We first investigated whether the hydroxy end groups of the linear PCL macroinitiators were able to initiate the bulk AROP of EP using DBU catalyst. Three PCL macroinitiators of different MW were utilized; specifically, a monohydroxy (Bz-PCL$_{19}$OH) and two dihydroxy telechelics (HO-PCL$_4$-OH and HO-PCL$_9$-OH). These were synthesized in scCO$_2$ using benzyl alcohol and 1,6-hexanediol as initiator, respectively, with Sn(Oct)$_2$ as catalyst (Table 1 and Table S1).[58] These first blocks were then extended through bulk polymerization of EP at a low-temperature (30-60 °C). For example, from the monofunctional Bz-PCL$_{19}$OH (M_n^{NMR} 2300 g/mol, Đ of 1.02) in the presence of DBU, we demonstrated high EP monomer conversions (~88-98% by ^{1}H NMR) at a temperature of 60 °C. This seemed to be the most suitable temperature to balance the increased viscosity and to drive the reaction to the desired conversion. Linear Bz-PCL$_{19}$-b-PEP$_{30}$ diblock copolymer was obtained with 92% conversion in only 2 h under these experimental conditions (Table 1, Entry 5).

Similarly, triblock copolymers were synthesized from OH-PCL$_4$-OH (M_n^{NMR} of 600 g/mol, Đ of 1.25, Table S1) and HO-PCL$_9$-OH (M_n^{NMR} of 1100 g/mol, Đ of 1.29, Table 1, Entry 2) macroinitiators at 60 °C and purified using supercritical CO$_2$ extraction and by dialysis (see SI).

In the following discussion, the linear diblock copolymer and triblock copolymers are denoted as Bz-PCL$_n$-b-PEP$_m$ and PEP$_{m/2}$-b-PCL$_n$-b-PEP$_{m/2}$ respectively, where n and m correspond to the number average of CL and EP units (Figure 2).
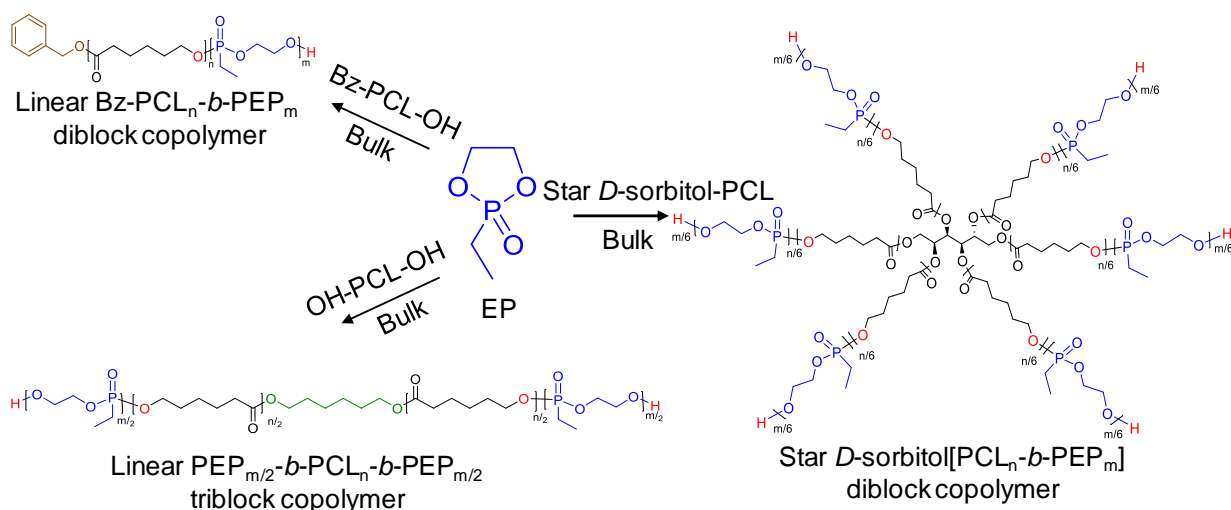
Figure 2. Schematic representation of the bulk AROP of EP from macroinitiators of various architecture using DBU as a catalyst. Linear monohydroxy Bz-PCL$_n$OH and dihydroxy OH-PCL$_n$-OH to afford linear Bz-PCL$_n$-b-PEP$_m$ diblock, linear PEP$_{m/2}$-b-PCL$_n$-b-PEP$_{m/2}$ triblock and star D-sorbitol[PCL$_n$-b-PEP$_m$] diblock copolymers.

Table 1. Analytical data for linear PCL$_n$-b-PEP$_m$ diblock, linear PEP$_{m/2}$-b-PCL$_n$-b-PEP$_{m/2}$ triblock and star diblock copolymers synthesized in the bulk using DBU as a catalyst at 60 °C.

Entry	Code [a]	[M]$_0$:[I]$_0$:[C]$_0$	Conv [e] (%)	t (h)	DP_n [f]	M_n^{NMR} [g] (g/mol) (macro-initiator)	M_n^{NMR} [h] (g/mol) (PEP block)	M_n^{Copoly} [i] (g/mol)	M_n^{SEC} (g/mol)	Đ
1	Bz-PCL$_{19}$OH	22:1:0.1[b]	90	3	19	2300	-	-	2600 [j]	1.02
2	HO-PCL$_9$-OH	9:1:0.1 [c]	99	0.5	8.8	1100	-	-	1000 [k]	1.29
3	D-sorbitol[PCL$_{57}$OH$_5$]OH	57:1:0.1[d]	99	62	57	6700	-	-	6700 [l]	1.04
4	D-sorbitol[PCL$_{18}$OH$_4$]OH$_2$	18:1:0.1 [d]	98	30	18	2200	-	-	3700 [l]	1.18
5	Bz-PCL$_{19}$-b-PEP$_{30}$	45:1:1 [e]	92	2	30	-	4100	6400	6400 [j]	1.04
6	PEP$_{7.2}$-b-PCL$_9$-b-PEP$_{7.2}$	16:1:0.5 [e]	98	2	14.5	-	2000	3100	1500 [k]	1.25
7	D-sorbitol[PCL$_{57}$-b-PEP$_{36}$OH$_6$]	46:1:6 [e]	89	5	36	-	4900	11600	12500 [l]	1.10
8	D-sorbitol[PCL$_{18}$-b-PEP$_{27}$OH$_6$]	38:1:6 [e]	89	5	27	-	3700	6000	6500 [j]	1.25

[a] Sample label, the subscripts represent the degree of polymerization of PCL and PEP blocks determined from ^{1}H NMR. [b,c,d] Molar ratio of [Monomer]$_0$:[Initiator]$_0$:[Catalyst]$_0$ based on DP_n^{targ} = [M]/[I] for macroinitiators with [b] [ε-CL]$_0$:[BzOH]$_0$: [Sn(Oct)$_2$]$_0$, [c] [ε-CL]$_0$:[HexD]$_0$:[Sn(Oct)$_2$]$_0$, [d] [ε-CL]$_0$:[D-sorbitol]$_0$:[Sn(Oct)$_2$]$_0$;
[e] [EP]$_0$:[macroinitiator]$_0$:[DBU]$_0$. [f] Determined by ^{1}H NMR after purification (after dialysis or after SCFE).
[g] M_n^{NMR} (macroinitiator) and M_n^{NMR} (PEP block) determined by ^{1}H NMR following eq. S1 and S3 respectively.
[i] M_n^{Copoly} is M_n^{NMR} (macroinitiator) + M_n^{NMR} (PEP block) (eq. S4)
[j] Determined by SEC (RI, Double Angle LS) in DMF at 45 °C from the dn/dc values of Bz-PCL$_{19}$OH (0.04 mL/g) and Bz-PCL$_{19}$-b-PEP$_{30}$ (0.026 mL/g).
[k] Determined via SEC (RI, PEG standard) in DMF at 50 °C.
[l] Determined via SEC (RI, PMMA standard) in DMF at 50 °C.

The SEC (RI, Double Angle LS) analysis confirmed the success of bulk copolymerization with a clear increase in the elution time and MW of the Bz-PCL$_{19}$-b-PEP$_{30}$ diblock compared to the Bz-PCL$_{19}$OH macroinitiator (Figure 3 (a)). Additionally, the copolymer obtained showed narrow dispersity (Đ= 1.04) (Table 1, Entry 5). $M_n^{SEC-\ DMF}$(RI, Double Angle LS) obtained using dn/dc of the corresponding polymers were in good agreement with those calculated from

the M_n^{NMR} values (Macroinitiator: $M_n^{SEC\text{-}DMF} = 2600$ g/mol vs. $M_n^{NMR} = 2300$ g/mol and diblock copolymer: $M_n^{SEC\text{-}DMF} = 6400$ g/mol vs. $M_n^{Copoly} = 6400$ g/mol) (Table 1, Entry 1 vs Entry 5).

The composition and the molecular weight of the copolymers were assessed with ^{1}H NMR and ^{31}P NMR; with all the characteristic resonances of macroinitiator Bz-PCL$_{19}$OH (Figure S1) and diblock Bz-PCL$_{19}$-*b*-PEP$_{30}$ copolymer (Figure 3b) assigned. These data also confirm the successful growth of the PEP block from the macroinitiator. For information, ^{1}H and ^{31}P NMR spectra of EP monomer are presented (Figure S2).
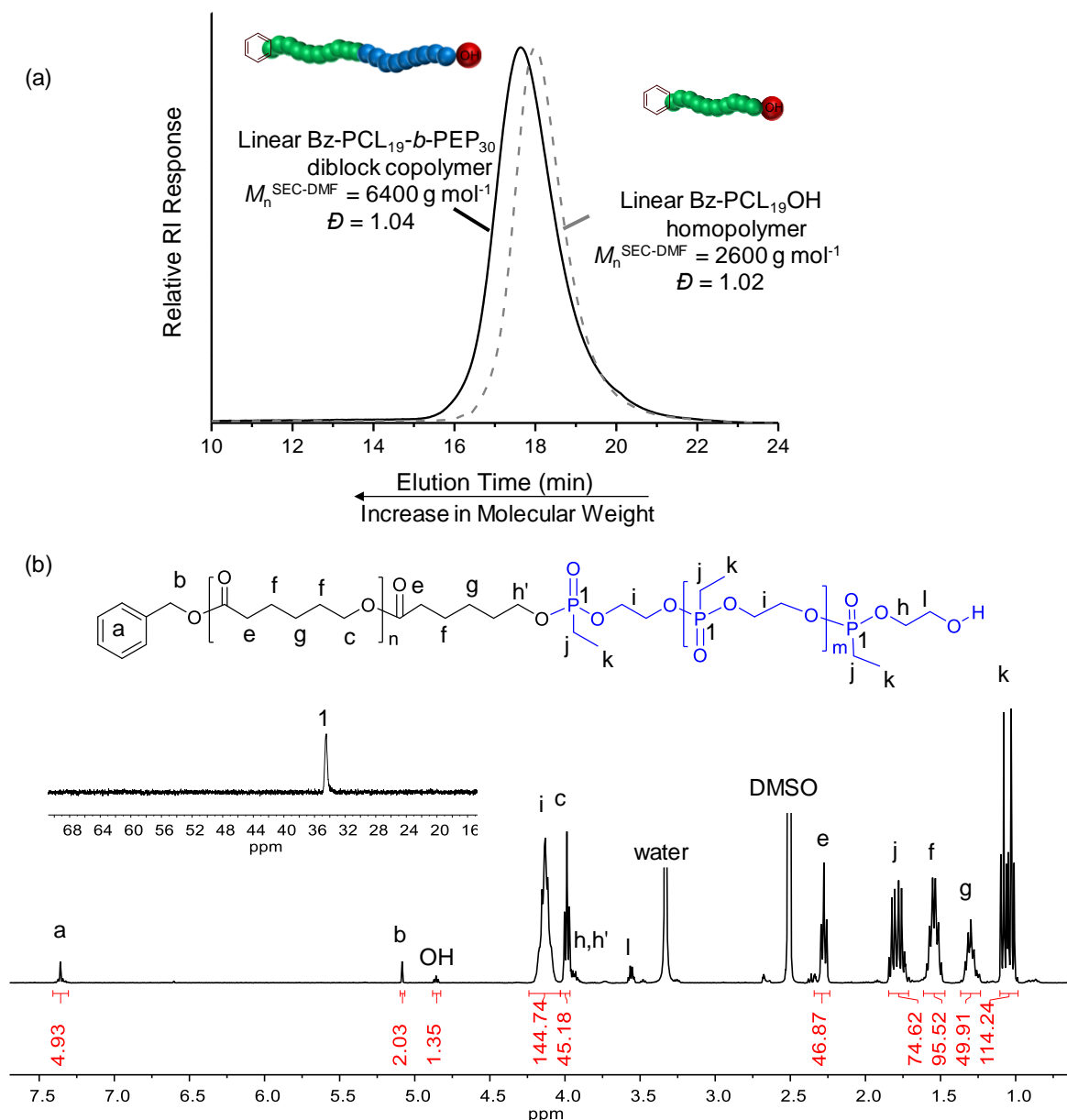

Figure 3. (a) SEC (RI, Double Angle LS) showing linear Bz-PCL$_{19}$OH macroinitiator synthesized using scCO$_2$ and the chain extension to the linear diblock Bz-PCL$_{19}$-*b*-PEP$_{30}$ (Table 1, Entry 1 vs Entry 5) and (b) ^{1}H NMR spectrum of the block copolymer and ^{31}P NMR inset (solvent DMSO-d_6).

Thus, ^{1}H NMR and SEC (RI, DALS) analyses confirm that there is indeed a covalent link between the PCL and PEP blocks and that the 'green' solvent-free bulk polymerization does produce copolymers with good control (Figure 3).

Having synthesized the block copolymers, the next task was to assess their surface-active properties and we began by looking at the solubility of the synthesized polymers in water. The Bz-PCL$_{19}$-b-PEP$_{30}$ copolymer gave a faint-cloudy suspension at 0.5 wt%. By contrast, homopolymer Bz-PCL$_{19}$OH was found to be totally insoluble in water which confirms the amphiphilic nature of this Bz-PCL$_{19}$-b-PEP$_{30}$ diblock copolymer. To modulate the solubility of any copolymer in water, the ratio of PEP: PCL should be varied by tuning the block lengths.[59] Indeed, when we increased the length of the PEP block, the linear block copolymer tended to solubilize more easily in water.
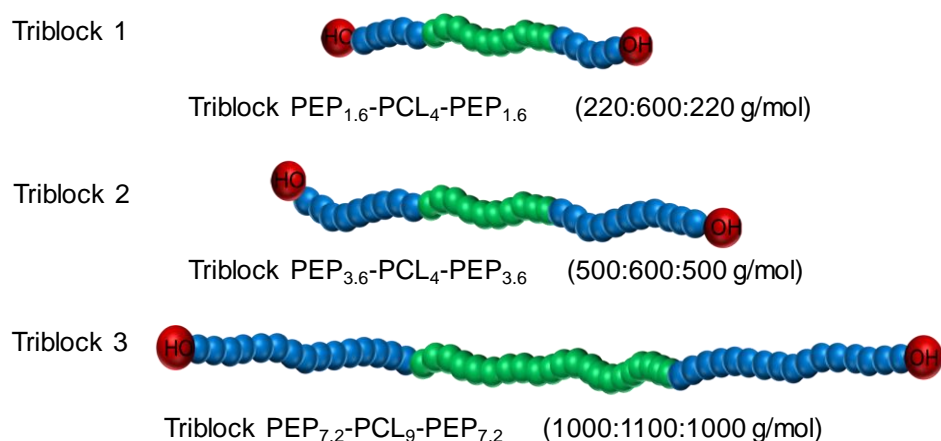

Triblock 1

Triblock PEP$_{1.6}$-PCL$_4$-PEP$_{1.6}$ (220:600:220 g/mol)

Triblock 2

Triblock PEP$_{3.6}$-PCL$_4$-PEP$_{3.6}$ (500:600:500 g/mol)

Triblock 3

Triblock PEP$_{7.2}$-PCL$_9$-PEP$_{7.2}$ (1000:1100:1000 g/mol)

Figure 4. Schematic of linear triblock PEP$_m$-PCL$_n$-PEP$_m$ (Triblock 1 -3) compounds with its variable molecular weight and composition where green symbols (🟢🟢🟢) represents PCL arms, blue (🔵🔵🔵) for PEP arms and red (🔴) for hydroxy end-groups.

Triblock copolymers, with a shorter central PCL hydrophobe (M_n^{NMR} (PCL) = 600 g/mol for HO-PCL$_4$-OH or M_n^{NMR} (PCL) =1100 g/mol for HO-PCL$_9$-OH) were explored. More precisely, two PEP$_{m/2}$-b-PCL$_n$-b-PEP$_{m/2}$ triblock amphiphiles with increasing proportion of PEP$_{m/2}$ blocks (for DP_n^{targ} (PCL$_n$) = 4 then DP_n^{targ} (PEP$_m$) ~5.3 and ~9.6) were synthesized (Table S1, Figure 4). Additionally, a third triblock copolymer was synthesized which nearly doubled both the hydrophilic PEP$_m$ and hydrophobic PCL$_n$ block (i.e., to increase the MW but maintained the same hydrophilic-lipophilic balance (HLB)). All the syntheses were conducted following protocols employed for diblock copolymer and analytical results and SEC plots are presented (Table 1, Table S1, and Figure S4).

3.1.2. Purification of Diblock and Triblock Copolymers using SCFE

It is well-known that purification of amphiphilic copolymers or surfactants is not straightforward and often multiple steps using volatile organic solvents are involved.[44] For instance, Wolf et al. reported that the precipitation of the homo polyphosphonate by cold diethyl ether gave a low yield (65 ± 2%) with traces of DBU detected by ^{1}H NMR.[50] As an alternative, purification by dialysis (molecular weight cut-off 1000 g/mol) against Milli-Q water was performed. We found that most of the DBU was separated from the sample but the yield (60 ± 5%) was not significantly improved, probably because of the low MW of the surfactants (~600-3500 g/mol). Also, dialysis is time-consuming and always requires an

energy-intensive freeze-drying step. Thus, we decided to explore the use of $scCO_2$ for purification, most notably for removal of solvent or monomer residues[60] noting that supercritical fluid extraction (SCFE) is commercially viable on the large scale[61,62] largely because CO_2 is an abundant, renewable and inexpensive resource.

SCFE was employed to purify copolymers formed in bulk reactions, primarily targeting removal of the $scCO_2$ soluble DBU organocatalyst and residual monomers. The $scCO_2$ insoluble polymers remain in the autoclave and can be easily collected. The $scCO_2$ extracted materials were collected via venting and analyzed by ^1H NMR (SI SCFE purification) and showed that ~11.5 wt% of EP monomer was extracted from the $PEP_{3.6}$-b-PCL_4-b-$PEP_{3.6}$ triblock amphiphile in just 25 min (Figure S3). The clear viscous liquid polymer was retrieved from the autoclave with high gravimetric yield (~92 ± 2%) and showed only traces of EP (0.5 wt%).

These data highlight that the use of $scCO_2$ dramatically improves the yield post purification (an increase of 42% was observed). In addition, comparing to other process, we can assume that this method is non toxic (no use of VOC), time saving (only 25 min to purify more than 2 g of polymer versus more than 6 h for less that 1 g by the dialysis method), energy saving (no drying or lyophilization step).

Additionally, the ^1H NMR spectrum of the material extracted by $scCO_2$ revealed that the cyclic EP ring remained intact after the purification process (Figure S3 (B)). In the dialysis-purification method this is not the case. Thus, $scCO_2$ might allow for recovery and recycling of the monomer, which would be desirable on the commercial scale and for the circular economy.

3.1.3. MALDI-TOF of PEP-b-PCL-b-PEP Triblock Copolymer

The MALDI-TOF data obtained from a representative $PEP_{7.2}$-b-PCL_9-b-$PEP_{7.2}$ triblock copolymer displays a monomodal Gaussian distribution (Figure 5) implying the presence of only a single series of peaks assigned to the triblock copolymer. No residual HO-PCL-OH macroinitiator was detected, thus confirming efficient synthesis via chain extension in the bulk.
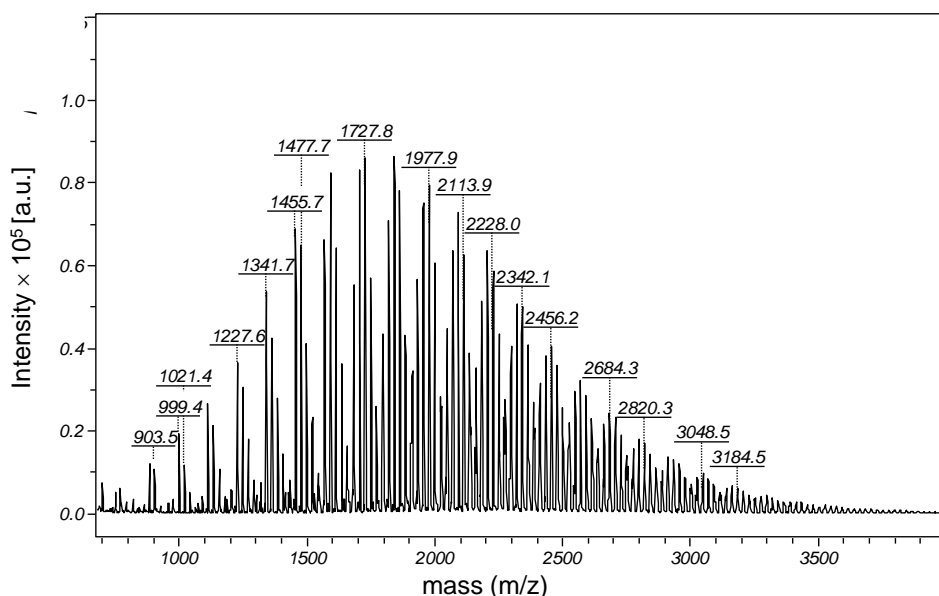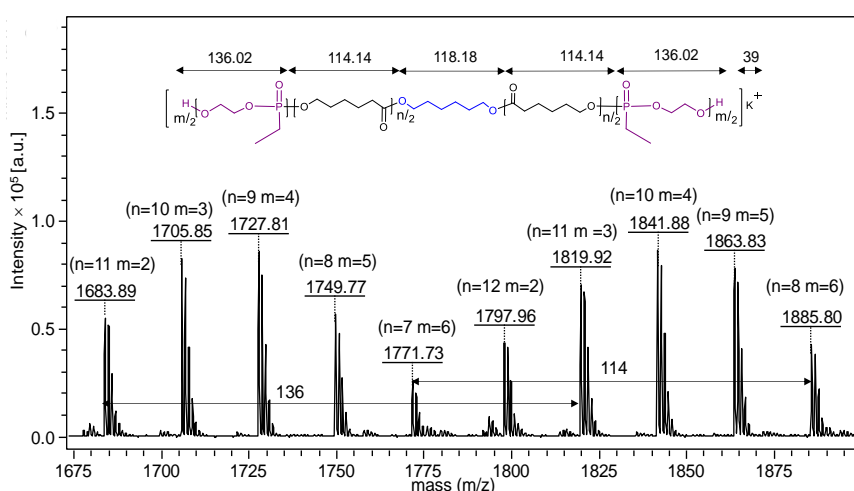
Figure 5. Full MALDI-TOF mass spectrum (reflection mode) of a PEP$_{7.2}$-*b*-PCL$_9$-*b*-PEP$_{7.2}$ triblock copolymer synthesized in the bulk in the presence of DBU and OH-PCL$_9$-OH as a macroinitiator (Table 1, Entry 6).

A more detailed analysis of the MALDI-TOF data in the region corresponding to the strongest peaks (1675 – 1900 m/z; Figure 6 and Table 2) shows each peak of the triblock copolymer arises from one central 1,6-hexanediol group (i.e. the initiator of the PCL blocks), some units of ε-CL and some units of EP monomer incremented with one potassium cation due to ionization. The number of repeating units of ε-CL (n) and EP (m) present in the copolymer was determined by comparing the experimental mass/charge ($(m/z)_{expt}$) values with the calculated monoisotopic mass/charge ($(m/z)_{calc}$) values (eq. 1):

$$(m/z)_{calc} = n_{\varepsilon\text{-CL}}\, M_{\varepsilon\text{-CL}} + m_{EP}\, M_{EP} + M_{1,6\text{-hexanediol}} + M_K$$

eq. 1

Figure 6. Enlarged MALDI-TOF mass spectrum (reflection mode) of a PEP$_{7.2}$-*b*-PCL$_9$-*b*-PEP$_{7.2}$ triblock copolymer synthesized in the bulk in the presence of DBU using OH-PCL$_9$-OH as a macroinitiator (Table 1, Entry 6). The structure and the masses of the triblock copolymer are presented for interpretation.

11

Table 2. Assignments of the peaks in PEP$_{7.2}$-b-PCL$_9$-b-PEP$_{7.2}$ triblock copolymers, with n ε-CL units and m EP units.

(m/z)$_{expt}$	n	m	(m/z)$_{calc}$[a]	Δ = (m/z)$_{calc}$ - (m/z)$_{expt}$
1683.89	11	2	1683.8692	-0.0208
1705.85	10	3	1705.8301	-0.0199
1727.81	9	4	1727.7910	-0.019
1749.77	8	5	1749.7518	-0.0182
1771.73	7	6	1771.7126	-0.0174
1797.96	12	2	1797.9373	-0.0227
1819.92	11	3	1819.8982	-0.0218
1841.88	10	4	1841.8591	-0.0209
1863.83	9	5	1863.8199	-0.0101
1885.79	8	6	1885.7807	-0.0093

[a] Calculated from the monoisotopic mass. The color-coded rows represent change of units (decreasing n and increasing m or vice-versa) in the series.

The MALDI-TOF spectrum of the copolymer shows the differences in the (m/z)$_{expt}$ series of peaks to be either 136.03 (m_{EP} = 136.02) (e.g. 1683.39 and 1819.92, 1705.85 and 1841.88 etc.), or 114.07 ($n_{\text{ε-CL}}$ = 114.14) (e.g. 1771.73 and 1885.80, 1797.96 and 1911.99 etc). All the (m/z)$_{expt}$ values for these series of peaks were in good correlation with the calculated (m/z)$_{calc}$ values (Table 2). Hence, the MALDI-TOF spectrum confirms the formation of the copolymer PEP$_m$-b-PCL$_n$-b-PEP$_m$ synthesized in the bulk using DBU as a catalyst. To the best of our knowledge, this is the first example of structural elucidation of phosphonate copolymers by MALDI-TOF-MS analysis.

3.2. Synthesis of Star PCL-b-PEP Diblock Amphiphilic Copolymers

After demonstrating the clean synthesis of linear diblock and triblock copolymers and their purification by SCFE we then moved on to attempt the synthesis of more complex star diblock copolymers using a renewable material, D-sorbitol as the core.

In this section we developed star homopolymer and diblock copolymers; referred as star D-sorbitol[PCL$_n$OH$_x$]OH$_y$ and star D-sorbitol[PCL$_n$-b-PEP$_m$OH$_x$]OH$_y$, respectively; where n, m and x correspond to the average amount of CL, EP and the average arm number on the PCL and y refers to the residual hydroxy groups on D-sorbitol (assessed by ^{31}P NMR phosphitylation).

Star D-sorbitol[PCL$_n$OH$_x$]OH$_y$ were produced by growing homopolymer PCL arms from D-sorbitol according to previous work.[58] Briefly, two samples with different PCL arm lengths (M_n^{targ} = 6700 g/mol and 2200 g/mol, Table 1, Entry 3-4) were prepared by synthesis in scCO$_2$ at 95 °C and 240 bar with Sn(Oct)$_2$ catalyst. Full conversion (98-99%) was achieved in 62 h and 30 h for star D-sorbitol[PCL$_{57}$OH$_5$]OH and star D-sorbitol[PCL$_{18}$OH$_4$]OH$_2$, respectively (Table 1, Entry 3-4). Star diblock copolymers comprising of PCL$_n$ hydrophobe and PEP$_m$ hydrophile were prepared from these star D-sorbitol[PCL$_{57}$OH$_5$]OH and star D-sorbitol[PCL$_{18}$OH$_4$]OH$_2$ as macroinitiators. Briefly, PEP block of different block lengths (M_n^{NMR} = 4900 g/mol and 3700 g/mol) were prepared in the bulk at 60 °C using DBU catalyst for 5 h to give 89% conv for both star D-sorbitol[PCL$_{57}$-b-PEP$_{36}$OH$_6$] and star D-sorbitol[PCL$_{18}$-b-PEP$_{27}$OH$_6$]

The ^{1}H NMR (DMSO-d_6) spectrum of star D-sorbitol[PCL$_{57}$-b-PEP$_{36}$OH$_6$] diblock copolymers showed resonances of PCL and PEP blocks (Figure 7, Table 1, Entry 7). Protons of D-sorbitol core were superseded by protons of the arms (Figure 7b).
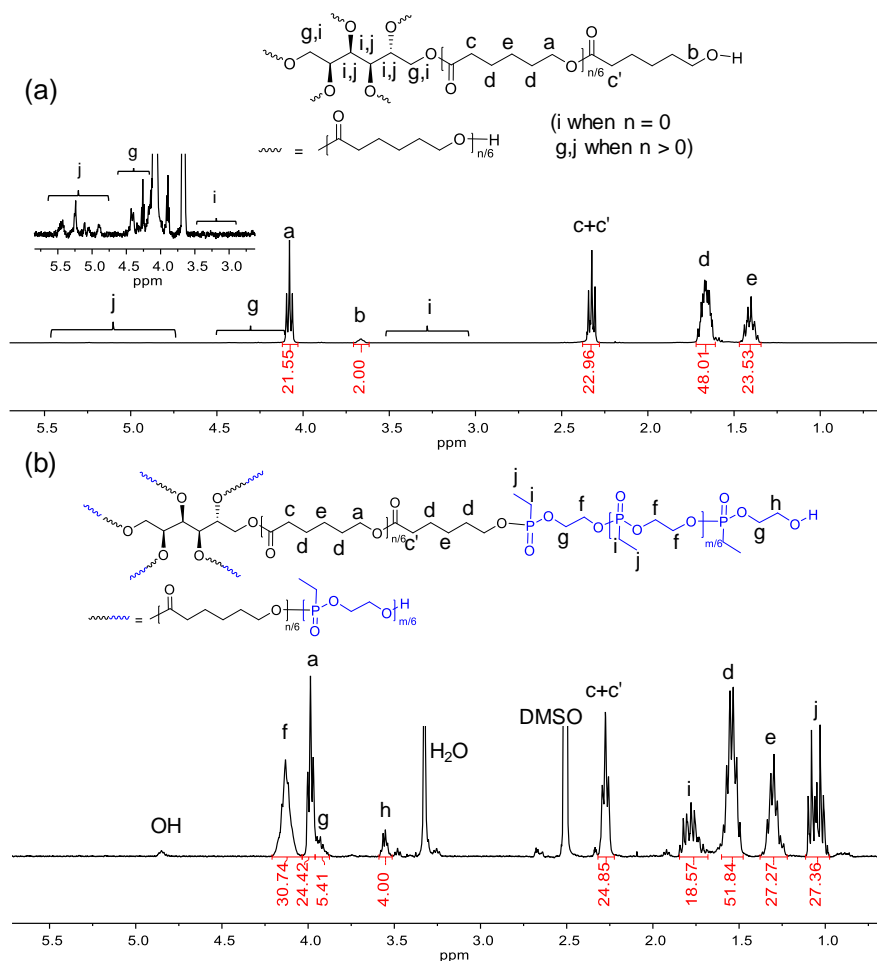
Figure 7. ^{1}H NMR spectra of (a) star D-sorbitol[PCL$_{57}$OH$_5$]OH macroinitiator (in CDCl$_3$) synthesized in scCO$_2$ (at 95 °C and 240 bar) using Sn(Oct)$_2$ and (b) the star D-sorbitol[PCL$_{57}$-b-PEP$_{36}$OH$_6$] diblock copolymer (in DMSO-d_6) synthesized in the bulk at 60 °C using DBU and purified using scCO$_2$ (Table 1, Entry 3 vs 7).

The resonance of the methylene protons (PCL−CH_2OH, **b**) at δ 3.66 ppm in the ^{1}H NMR of the macroinitiator (Figure 7a) disappears in the star diblock copolymer spectrum (Figure 7b) and is replaced by a new resonance appearing downfield at δ 3.56 ppm attributed to the hydroxymethyl end-group (PEP−OP(=O)−O−CH$_2$−CH_2−OH, **h**). These data imply that the EP units have grown from the hydroxy end-groups of the star PCL. From the ^{1}H NMR spectrum, DP^{NMR} (PEP block) is shown to be 36 (from eq. S2), M_n^{NMR} (PEP block) of 4900 g/mol (eq. S3) and M_n^{Copoly} of 11600 g/mol (eq. S4) were estimated for star D-sorbitol[PCL$_{57}$-b-PEP$_{38}$OH$_6$] (Table 1, Entry 7, Figure 7).

Furthermore, SEC (RI, PMMA standard) analysis in DMF, clearly shows an increase in elution time, an increase in MW and a monomodal dispersity ($Đ$ = 1.10) for star D-sorbitol[PCL$_{57}$-b-PEP$_{36}$OH$_6$] (Figure 8, Table 1, Entry 7). The data also indicate that there is no residual PCL homopolymer signal. The SEC data generated using PMMA calibration were slightly overestimated in comparison to ^{1}H NMR values for star D-sorbitol[PCL$_{57}$OH$_5$]OH ($M_n^{SEC-DMF}$ 8300 g/mol vs. M_n^{Copoly} 6700 g/mol) and star D-sorbitol[PCL$_{57}$-b-PEP$_{36}$OH$_6$] diblock

copolymer ($M_n^{SEC-DMF}$ 12500 g/mol vs. M_n^{Copoly} 11600 g/mol) prepared in the bulk (Table 1, Entry 3 vs Entry 7).
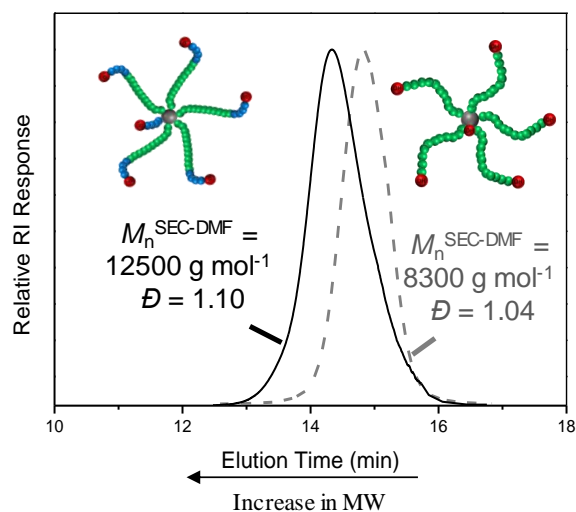

Figure 8. SEC (RI, PMMA standard) traces of star D-sorbitol[PCL$_{57}$OH$_5$]OH synthesized in scCO$_2$ (at 95 °C and 240 bar) using Sn(Oct)$_2$ and the corresponding star D-sorbitol[PCL$_{57}$-b-PEP$_{36}$OH$_6$] diblock copolymer synthesized in the bulk using DBU at 60 °C (Table 1, Entry 3 vs 7).

These results highlight that high MW amphiphilic star diblock copolymers ($M_n^{SEC-DMF}$ ~ 12500 g/mol) with narrow dispersity ($Đ = 1.10$) can be synthesized in the bulk in the absence of VOCs. The polymer end-groups were precisely identified by phosphitylation using a phospholane reagent[58]. This confirmed that all the end-groups of star D-sorbitol-PCL were utilized to radiate PEP arms, indicating formation of 6 arms with at least 5 amphiphilic arms (Figure 9, Figure S5)
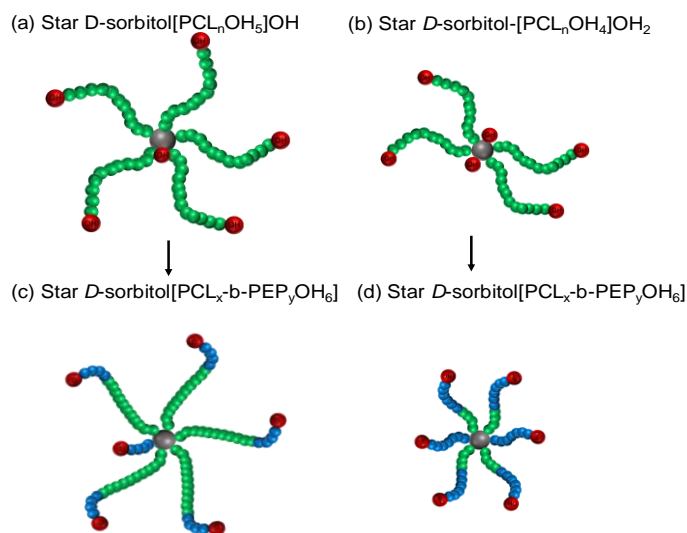

Figure 9. Representations of star D-sorbitol-PCL synthesized with Sn(Oct)$_2$; (a) 5 −PCL arms and 1 −OH on D-sorbitol (M_n^{NMR} (PCL) = 6700 g/mol); (b) 4 −PCL arms and 2 −OH on D-sorbitol (M_n^{NMR} (PCL) 2240 g/mol). The corresponding star D-sorbitol[PCL-b-PEP] (c) 5 −PCL-b-PEP arms and 1−PEP arm on D-sorbitol (M_n^{Copoly} = 11600 g/mol), and (d) 4 −PCL-b-PEP arms and 2 −PEP arms on D-sorbitol (M_n^{Copoly} = 6000 g/mol). The D-sorbitol core (●), PCL arms (●●●), PEP arms (●●●) and hydroxyl groups (●) are presented.

14

Linear diblock and triblock copolymers as well as star diblock copolymers were successfully synthesized by AROP of EP from linear and star PCL-based macroinitiators. Such amphiphilic copolymers could be surface active and able to self-assemble in aqueous solution, two key parameters for surfactant characterization.

3.3 Surface Activity of Linear and Star PCL-*b*-PEP Block Copolymers

We investigated the surface activity of the building blocks and the synthesized compounds. A compound that reduces the surface tension (γ) of water from 72 mN/m to below $\leq$ 60 mN/m can be classed as a surfactant.[60]

The starting materials, *D*-sorbitol (core) and EP monomer do not reduce the surface tension and nor does the linear Bz-PCL$_{19}$-*b*-PEP$_{30}$. The first star compound *D*-sorbitol[PCL$_{57}$-*b*-PEP$_{36}$OH$_6$] forms a cloudy solution under ambient condition at 5 wt% (Table 1, Entry 4 and Entry 7) but has no effect on surface tension. We speculate that this is a result of the longer length of hydrophobic ε-CL compared to only a short hydrophilic PEP unit.

In sharp contrast, the star counterpart *D*-sorbitol[PCL$_{18}$-*b*-PEP$_{27}$OH$_6$] showed a significant effect upon surface tension lowering to 45 mN/m (Figure S6, Table 1, Entry 5 vs. 8). These results are promising when compared with commercial oil-based and non-degradable surfactants (Tween 20 and 80) where the values ranged between 32-40 mN/m (Figure S6).

The triblock copolymers were all soluble in water and showed surface tension in the range 38-40 mN/m (Figure 10, Table S2). Interestingly, the linear PEP$_{7.2}$-*b*-PCL$_9$-*b*-PEP$_{7.2}$ triblock copolymer (PEP:PCL:PEP 1000:1100:1000 g/mol) showed the lowest surface tension at γ = 31.7 mN/m; lower than commercial Pluronic ^{TM} with γ values from 40-49 mN/m (Figure 10).
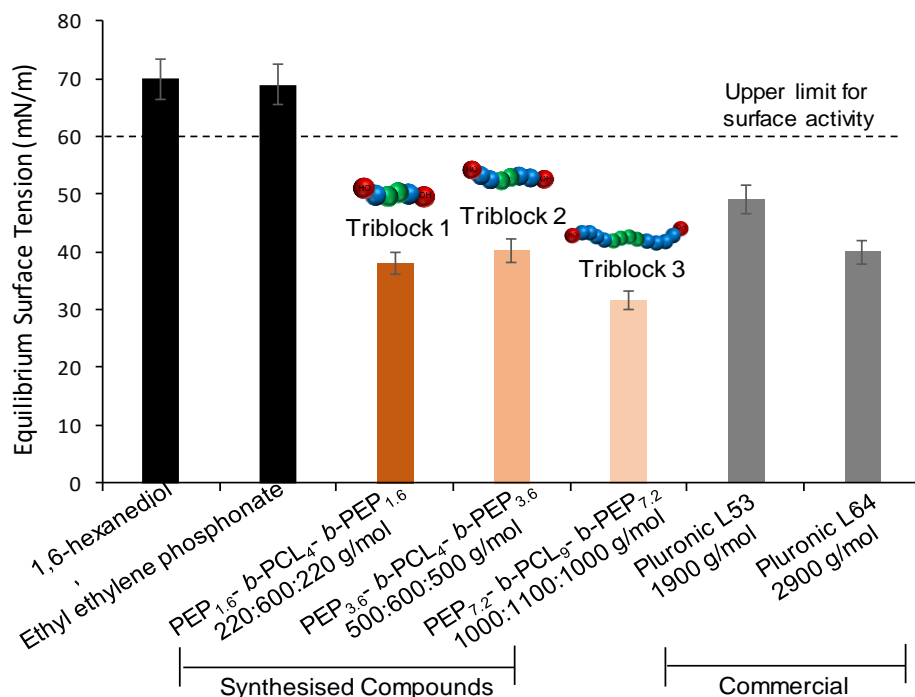

Figure 10. Representation of linear triblock PEP$_m$-PCL$_n$-PEP$_m$ compounds with its different molecular weight and composition. The PCL arms (●), PEP arms (●) and hydroxy groups (●) are presented; (bottom) equilibrium surface tension values of 1,6 hexanediol and ethyl ethylene phosphonate building blocks (black bars) and synthesised triblock PEP$_m$-*b*-PCL$_n$-*b*-PEP$_m$ copolymers of variable MW and compositions (brown bars) measured against commercial triblock surfactants, Pluronic.

To simplify the self-assembly and surface activity discussion, these copolymers are grouped based on MW with low, intermediate and high MW copolymer (Table S3).

3.4. Self-assembly of linear triblock and star diblock PCL-*b*-PEP copolymers

3.4.1. CAC of triblock and star amphiphilic copolymers

The Critical aggregation concentration (CAC) of the triblock $PEP_{7.2}$-*b*-PCL_9-*b*-$PEP_{7.2}$ (Triblock 3) was measured using the Wilhelmy plate method. Theoretically, the sequential addition of triblock surfactant into water will decrease surface tension as more surfactant accumulates at the air/water interface. Only when the interface becomes saturated does further addition of surfactant lead to aggregation/micellization. All the triblock copolymers behaved in a similar manner. A sharp change in the slope was identified from the point where the two regression lines intersect to give a concentration of 47.9 µM (0.014 wt%) for the CAC (Figure S7). Above the CAC, the surface tension remained ~34 mN/m. For the star copolymer, a similar analysis showed a concentration of 21.2 µM (0.012 wt%) for the CAC (Figure S8).

We chose two points above the CAC (0.1 and 0.5 wt%) to study the self-assembly of aqueous solutions of all the amphiphiles.

3.4.2. Self-assembly of linear triblock copolymers

For the triblock copolymers, the auto-correlation functions of the low MW triblock copolymers showed two or three distinct populations of nanoparticles in the intensity-weighted distributions. (Figure 11, upper; Table 1 & Table S3). These samples were studied without filters to give a full picture of the range of populations present. As always with DLS it is important to note that scattering is much more sensitive to larger objects[63] as shown in the intensity-weighted distributions (Figure 11, upper) whereas the number distributions (Figure 11, lower) give a more realistic picture showing that these particles are insignificant in terms of the number-weighed distribution.
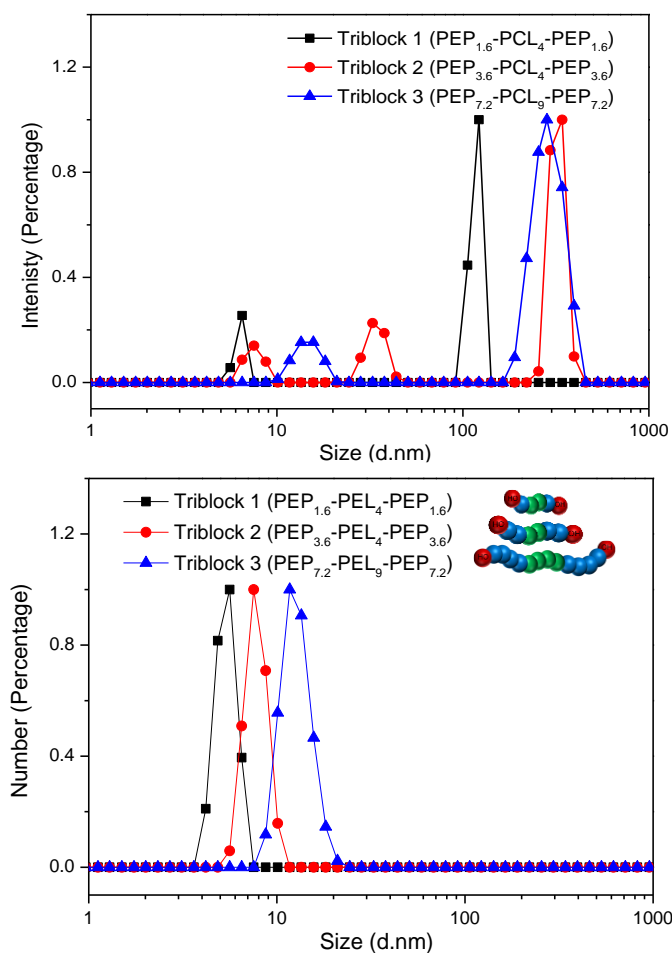
Figure 11. Intensity-weighted (upper) and Number-weighted (lower) size distributions of low MW PEP_m-b-PCL_n-b-PEP_m triblock amphiphiles directly dissolved in water at 0.1 wt% concentration. DLS measurements interpreted according to the CONTIN analysis at an angle of 173°.

The number-weighted distributions gave only one size distribution population for each of the triblocks with hydrodynamic diameters (D_H) from 5.6 to 14.5 nm (Figure 11, lower). As expected, the D_H-value increases from Triblock 1 (D_H = 5.6 nm) to Triblock 2 (D_H = 7.4 nm) because of the increased size of the PEP shell. Similarly, D_H also increases from Triblock 2 to Triblock 3 and all of these D_H-values most likely correspond to micelles. Theoretically, the size of a triblock ($PEP_{7.2}$-b-PCL_9-b-$PEP_{7.2}$) unimer should be around 3.5 nm assuming a condensed PCL_9 chain linked to two PEP_7 chains in a mushroom conformation. Comparing this with the observed $D_{H, DLS}$ = 14.5 nm infers a significant 71-fold increase of volume ($14.5^3/3.5^3$) compared to the unimer. The IWD data also show larger secondary and tertiary objects with D_H values 35 to 100-283 nm (Figure 11, top).

3.4.3. Intermediate MW Linear vs. Star Diblock Copolymers

The influence of the block copolymer architecture on self-assembly was further investigated by comparing the aqueous solutions of star D-sorbitol[PCL_{18}-b-$PEP_{27}OH_6$] (Table 1 entry 8) (hydrophilicity = 12.3) with its linear counterpart which is the diblock Bz-PCL_{19}-b-PEP_{30} (hydrophilicity = 12.8) (Table 1 entry 5) by DLS (at 0.1 and 0.5 wt%, directly dissolved in water (Table S3).

The linear diblock Bz-PCL$_{19}$-b-PEP$_{30}$ gave a turbid solution at the higher concentration (0.5 wt%) and so only 0.1 wt% was investigated and this showed a broad monomodal distribution (D_H-value = 145 nm in both intensity and number weighted plots (Figure 12)). By contrast, star D-sorbitol[PCL$_{18}$-b-PEP$_{27}$OH$_6$] was fully water soluble at 0.5 wt%, reflecting the influence of topology on solubility and self-assembly. The star copolymer showed a bimodal size distribution at 0.5 wt% with a primary population of smaller nanoparticles ($D_{H, DLS}$ = 7 nm) coexisting with larger aggregates ($D_{H, DLS}$ = 111 nm) (Figure 12, top). Importantly, the size distribution of the objects remains unchanged at the lower conc. (0.1 wt%) ($D_{H, DLS}$ = 6.3 and 107 nm). Water is a good solvent for the hydrophilic PEP blocks which will extend, and a poor solvent for the hydrophobic PCL block which will shrink. Thus, we would expect the theoretical size for D-sorbitol[PCL$_{18}$-b-PEP$_{27}$OH$_6$] to be about ~5 nm, assuming a fully extended chain conformation with six PEP$_{4.5}$ arms forming a corona around the condensed PCL$_{18}$ core. Since the DLS experiments were performed at 0.1 and 0.5 wt%, values above the CAC (0.012 wt%) (Figure S8), it is reasonable to conclude that the smallest observed diameter (D_H ~7 nm) corresponds to star unimers (Figure 12).

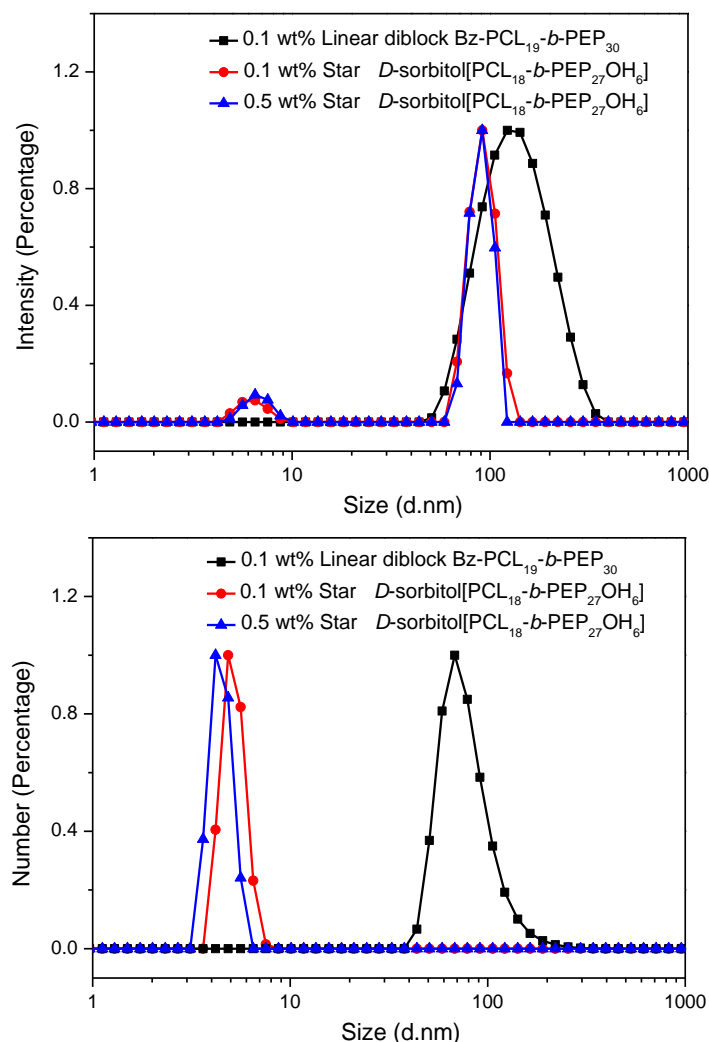**Figure 12**. Intensity-weighted (upper) and Number-weighted (lower) size distributions DLS results obtained for star D-sorbitol[PCL$_{18}$-b-PEP$_{27}$OH$_6$] (2200:3700) g/mol amphiphile and its linear analogues, linear diblock Bz-PCL$_{19}$-b-PEP$_{30}$ (2300: 4100) g/mol directly dissolved\ in water at 0.1 wt% concentration (Table 1, Entry 5 and Entry 8).

Bigger D_H-values observed by IWD may reasonably be attributed to a small population of aggregates of a few star unimers (Figure 12, upper) since the number-weighted distributions showed only monomodal distributions around 4.85 nm (Figure 12, lower).

3.4.4. High MW Star PCL-*b*-PEP Diblock Copolymers: Direct Dissolution vs. Nanoprecipitation Method

The large, high MW star copolymer star D-sorbitol[PCL$_{57}$-*b*-PEP$_{36}$OH$_6$] (Table 1 entry 7) showed reasonable hydrophilicity of 8.4 (Table S3, Entry 6) and so its self-assembly was attempted by direct dissolution in water. However, an aqueous solution of it displayed cloudiness even at the lower conc. 0.1 wt%. DLS results revealed co-existence of two populations (Figure S9, last vertical bars) with D_H-values of 19 and 142 nm in the intensity weighed-distribution. These larger aggregates and the observed turbidity led us to examine nanoprecipitation to perhaps yield smaller objects.

Briefly, in nanoprecipitation method the star samples (high MW star D-sorbitol[PCL$_{57}$-*b*-PEP$_{36}$OH$_6$], Table S3) were dissolved in acetone (a good solvent for both the PCL and PEP blocks), and self-assembly was induced by gradually adding the acetone solutions into Milli-Q water followed by vacuum removal of acetone.[64] The resultant aqueous solutions were transparent and DLS showed larger objects by intensity distribution $D_{H, DLS (IWD)}$ 240 nm in addition to smaller population ($D_{H, DLS (IWD)}$ 18 nm) but number distribution showed only single population with D_H of 13 nm (Figure S10).

As a control, the self-assembly of hydrophobic star D-sorbitol[PCL$_n$OH$_x$]OH samples (at 0.1 wt%) were studied in parallel following the nanoprecipitation method. These were found to be cloudy suggesting the hydroxyl groups alone on the PCL chains are incapable of stabilizing the hydrophobic PCL and hence it precipitates.

3.4.5. TEM and Cryo-TEM images of Star PCL-*b*-PEP Diblock Copolymers

The morphology of the star D-sorbitol[PCL$_{57}$-*b*-PEP$_{36}$OH$_6$] copolymer prepared by nanoprecipitation into the water was investigated by transmission electron microscopy (TEM). The TEM images show uniform size spheres (Figure S11 and Figure S12). The average particle diameter measured by TEM (D_{TEM}) was found to be smaller than the hydrodynamic diameter found by DLS (D_{TEM} = 14.3 nm and $D_{H, DLS (IWD)}$ = 18 nm) (Figure S12, histogram and Figure S10). This is exactly as one would expect since the TEM values are always slightly smaller because the aggregates are in their dry state whereas DLS measures the hydrated and swollen particles. Though in this case, the difference is actually relatively small suggesting limited shrinkage. The absence of the much larger aggregates on TEM images is not surprising as it reinforces the fact that these are overemphasized in the intensity weighted DLS measurements. (Figure S11 and Figure S12).

Cryo-TEM analyses of star D-sorbitol[PCL$_{57}$-*b*-PEP$_{36}$OH$_6$] in the native frozen-hydrated state (Figure 13) showed scattered spherical particles with an average $D_{cryo-TEM}$ of 17.7 nm. Values that are in excellent accordance with the DLS measurements ($D_{H, DLS (IWD)}$ = 18 nm).
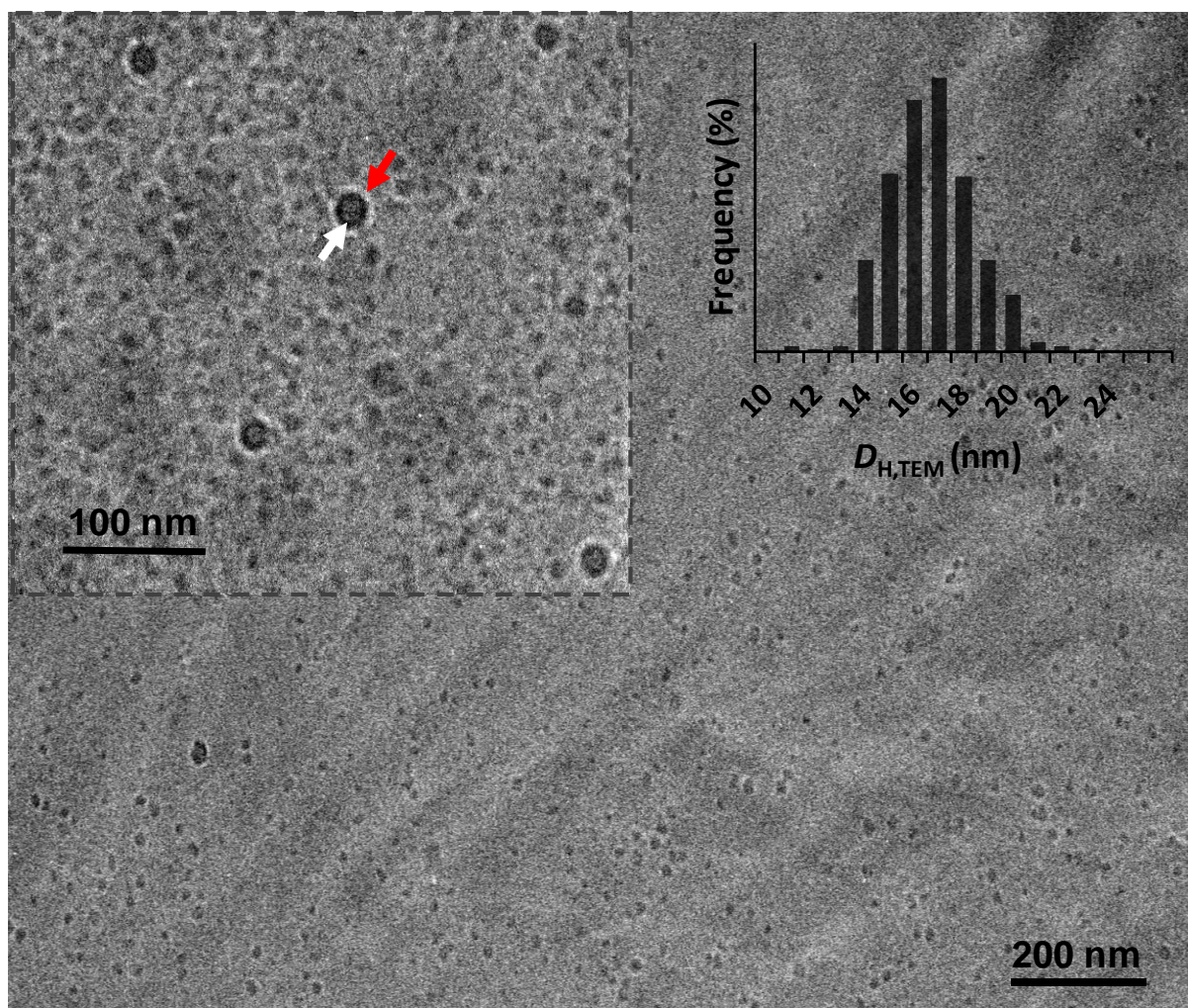
Figure 13. Cryo-TEM micrograph and size distribution histogram (analyzed using ImageJ software) of spherical nanoparticles formed by star *D*-sorbitol[PCL_{57}-*b*-$PEP_{36}OH_6$] diblock copolymer in aqueous solution (0.1 wt%) prepared by the nanoprecipitation method. The scale bar is 200 nm. Images obtained without staining (Table 1, Entry 7). The two arrows show PEP corona.

Spherical morphologies have been frequently reported for unimers of star-like and dendrimer structures.[8,12,15,17] Looking closely at the cryo-TEM, the grey core clearly shows the condensed and water-free PCL core (Inset of Figure 13). Whilst the white outer rings show the PEP in the corona diluted by water (arrowed red). The unusual dark black rings at the interface (arrowed white) might relate to a high concentration of phosphorus that has collapsed into a PEP segment at the interface between the PCL core and the PEP corona. This could happen where the water concentration is low.[65]

4. Conclusion

We present the first synthesis of linear diblock, triblock and star diblock copolymers utilising renewable and degradable PCL cores with degradable, hydrophilic poly(phosphonates). We utilized only renewable building-blocks of 1,6-hexanediol, *D*-sorbitol and ε-CL monomer and we demonstrate effective use of solvent-free bulk and clean scCO$_2$ based polymerisation systems to yield clean residue-free products. The triblocks show excellent activity as surfactants reducing the surface tension of water to a level that competes with the commercial Pluronic ^{TM} surfactants. The star diblock copolymers were shown to self-assemble in aqueous solvents yielding structures of ideal size for application in drug delivery or indeed a wide range of other possibilities. The demonstration of the utility of poly(phosphonates) as the hydrophile in these surfactants also opens up the possibility of replacing poly(ethylene glycol), the industry gold standard that is non-degradable and has recently been shown to bioaccumulate.

5. References

1   Global Surfactants Market 2018 - Segmented by Origin, Type, Application, Geography-Growth, Trends and Forecasts to 2023.

2   M. L. Adams, A. Lavasanifar and G. S. Kwon, *J. Pharm. Sci.*, 2003, **92**, 1343–1355.

3   L. Zhang and A. Eisenberg, *Science (80-.).*, 1995, **268**, 1728–1731.

4   A. Discher, D. E. & Eisenberg, *Science (80-.).*, 2002, **297**, 967–973.

5   K. Kataoka, A. Harada and Y. Nagasaki, *Adv. Drug Deliv. Rev.*, 2001, **47**, 113–131.

6   G. Gaucher, M. H. Dufresne, V. P. Sant, N. Kang, D. Maysinger and J. C. Leroux, *J. Control. Release*, 2005, **109**, 169–188.

7   M. Shibata, M. Matsumoto, Y. Hirai, M. Takenaka, M. Sawamoto and T. Terashima, *Macromolecules*, 2018, **51**, 3738–3745.

8   X. Pang, L. Zhao, M. Akinc, J. K. Kim and Z. Lin, *Macromolecules*, 2011, **44**, 3746–3752.

9   P. Alexandridis, *Curr. Opin. Colloid Interface Sci.*, 1996, **1**, 490–501.

10   Y. Wang and S. M. Grayson, *Adv. Drug Deliv. Rev.*, 2012, **64**, 852–865.

11   A. L. Sisson, D. Ekinci and A. Lendlein, *Polym. (United Kingdom)*, 2013, **54**, 4333–4350.

12   Z. Jia, Y. Zhou and D. Yan, *J. Polym. Sci. Part A Polym. Chem.*, 2005, **43**, 6534–6544.

13   P. Chmielarz, *Polymer (Guildf).*, 2016, **102**, 192–198.

14   T. Higashihara, M. Hayashi and A. Hirao, *Prog. Polym. Sci.*, 2011, **36**, 323–375.

15   Y. Wang, G. Qi and J. He, *ACS Macro Lett.*, 2016, **5**, 547–551.

16   X. Fan, Z. Li and X. J. Loh, *Polym. Chem.*, 2016, **7**, 5898–5919.

17   X. Yang, J. J. Grailer, S. Pilla, D. a Steeber and S. Gong, *Bioconjug. Chem.*, 2010, **21**, 496–504.

18   A. W. Bosman, H. M. Janssen and E. W. Meijer, *Chem. Rev.*, 1999, **99**, 1665–1688.

19   W. Lin, C. Yang, Z. Xue, Y. Huang, H. Luo, X. Zu, L. Zhang and G. Yi, *J. Colloid Interface Sci.*, 2018, **528**, 135–144.

20   A. Heise, J. L. Hedrick, C. W. Frank and R. D. Miller, *J. Am. Chem. Soc.*, 1999, **121**, 8647–8648.

21   Y. Mai, Y. Zhou and D. Yan, *Macromolecules*, 2005, **38**, 8679–8686.

22   C. Gao and D. Yan, *Prog. Polym. Sci.*, 2004, **29**, 183–275.

23   X. Jin, P. Sun, G. Tong and X. Zhu, *Biomaterials*, 2018, 1–13.

24   R. Dong, Y. Zhou, X. Huang, X. Zhu, Y. Lu and J. Shen, *Adv. Mater.*, 2015, **27**, 498–526.

25   J. M. Ren, T. G. McKenzie, Q. Fu, E. H. H. Wong, J. Xu, Z. An, S. Shanmugam, T. P. Davis, C. Boyer and G. G. Qiao, *Chem. Rev.*, 2016, **116**, 6743–6836.

26   P. Grossen, D. Witzigmann, S. Sieber and J. Huwyler, *J. Control. Release*, 2017, 260, 46–60.

27   K. Kono, C. Kojima, N. Hayashi, E. Nishisaka, K. Kiura, S. Watarai and A. Harada, *Biomaterials*, 2008, **29**, 1664–1675.

28   S. Chen, X.-Z. Zhang, S.-X. Cheng, R.-X. Zhuo and Z.-W. Gu, *Biomacromolecules*, 2008, **9**, 2578–2585.

29   B. Vyas, S. A. Pillai, A. Bahadur and P. Bahadur, *Polymers (Basel).*, , DOI:10.3390/polym10010076.

30   H. Claesson, E. Malmström, M. Johansson and A. Hult, *Polymer (Guildf).*, 2002, **43**, 3511–3518.

31   W.-J. Song, J.-Z. Du, N.-J. Liu, S. Dou, J. Cheng and J. Wang, *Macro*, 2008, **41**, 6935–6941.

32   K. H. Kim, G. H. Cui, H. J. Lim, J. Huh, C.-H. Ahn and W. H. Jo, *Macromol. Chem. Phys.*, 2004, **205**, 1684–1692.

33   J. Ulbricht, R. Jordan and R. Luxenhofer, *Biomaterials*, 2014, **35**, 4848–4861.

34   I. Hamad, A. C. Hunter, J. Szebeni and S. M. Moghimi, *Mol. Immunol.*, 2008, **46**, 225–232.

35   K. Knop, R. Hoogenboom, D. Fischer and U. S. Schubert, *Angew. Chemie Int. Ed.*, 2010, **49**, 6288–6308.

36   D. A. Herold, K. Keil and D. E. Bruns, *Biochem. Pharmacol.*, 1989, **38**, 73–76.

37   B. Romberg, J. M. Metselaar, L. Baranyi, C. J. Snel, R. Bünger, W. E. Hennink, J. Szebeni and G. Storm, *Int. J. Pharm.*, 2007, **331**, 186–189.

38   C. Li and S. Wallace, *Adv. Drug Deliv. Rev.*, 2008, **60**, 886–898.

39   L. Korchia, V. Lapinte, C. Travelet, R. Borsali, J.-J. Robin and C. Bouilhac, *Soft Matter*, 2017, **13**, 4507–4519.

40   C. V. de Macedo, M. S. da Silva, T. Casimiro, E. J. Cabrita and A. Aguiar-Ricardo, *Green Chem.*, 2007, **9**, 948–953.

41   R. Luxenhofer, Y. Han, A. Schulz, J. Tong, Z. He, A. V. Kabanov and R. Jordan, *Macromol. Rapid Commun.*, 2012, **33**, 1613–1631.

42   B. Verbraeken, B. D. Monnery, K. Lava and R. Hoogenboom, *Eur. Polym. J.*, 2017, **88**, 451–469.

43   R. Luxenhofer, A. Schulz, C. Roques, S. Li, T. K. Bronich, E. V. Batrakova, R. Jordan and A. V. Kabanov, *Biomaterials*, 2010, **31**, 4972–4979.

44   D. Rayeroux, V. Lapinte and P. Lacroix-Desmazes, *J. Polym. Sci. Part A Polym. Chem.*, 2012, **50**, 4589–4593.

45   C. Fetsch and R. Luxenhofer, *Polymers (Basel).*, 2013, **5**, 112–127.

46   C. Fetsch and R. Luxenhofer, *Macromol. Rapid Commun.*, 2012, **33**, 1708–1713.

47   R. Luxenhofer, C. Fetsch and A. Grossmann, *J. Polym. Sci. Part A Polym. Chem.*, 2013, **51**, 2731–2752.

48   T. Steinbach and F. R. Wurm, *Angew. Chemie Int. Ed.*, 2015, **54**, 6098–6108.

49   J. Simon, T. Wolf, K. Klein, K. Landfester and F. R. Wurm, 2018, 5548–5553.

50   T. Wolf, T. Steinbach and F. R. Wurm, *Macromolecules*, 2015, **48**, 3853–3863.

51   T. Steinbach, S. Ritz and F. R. Wurm, *ACS Macro Lett.*, 2014, **3**, 244–248.

52   K. N. Bauer, H. T. Tee, M. M. Velencoso and F. R. Wurm, *Prog. Polym. Sci.*, 2017, **73**, 61–122.

53   M. Richards, B. I. Dahiyat, D. M. Arm, P. R. Brown and K. W. Leong, *J. Biomed. Mater. Res.*, 1991, **25**, 1151–1167.

54   W. Mabey and T. Mill, *J. Phys. Chem. Ref. Data*, 1978, **7**, 383–415.

55   K. N. Bauer, L. Liu, M. Wagner, D. Andrienko and F. R. Wurm, *Eur. Polym. J.*, 2018, **108**, 286–294.

56   J. Beament, T. Wolf, J. C. Markwart, F. R. Wurm, M. D. Jones and A. Buchard, *Macromolecules*, 2019, **52**, 1220–1226.

57   F. C. Loeker, C. J. Duxbury, R. Kumar, W. Gao, R. A. Gross and S. M. Howdle, *Macromolecules*, 2004, **37**, 2450–2453.

58   P. Baheti, O. Gimello, C. Bouilhac, P. Lacroix-Desmazes and S. M. Howdle, *Polym. Chem.*, 2018, 5594–5607.

59   N. Kumar and R. Tyagi, *J. Dispers. Sci. Technol.*, 2014, **35**, 205–214.

60   A. R. Goddard, S. Pérez-Nieto, T. M. Passos, B. Quilty, K. Carmichael, D. J. Irvine and S. M. Howdle, *Green Chem.*, 2016, **18**, 4772–4786.

61   E. O. Goodship, Vannessa and Ogur, *Polymer Processing with Supercritical Fluids*, Rapra Technology Ltd, Shawbury, UK, 2004, vol. 15.

62   E. J. Beckman, *J. Supercrit. Fluids*, 2004, **28**, 121–191.

63   K. Loos, A. Böker, H. Zettl, M. Zhang, G. Krausch and A. H. E. Müller, *Macromolecules*, 2005, **38**, 873–879.

64   D. Kakde, V. Taresco, K. K. Bansal, E. P. Magennis, S. M. Howdle, G. Mantovani, D. J. Irvine and C. Alexander, *J. Mater. Chem. B*, 2016, **4**, 7119–7129.

65   Y. Y. Won, A. K. Brannan, H. T. Davis and F. S. Bates, *J. Phys. Chem. B*, 2002, **106**, 3354–3364.